

Nature of Brittle Fracture in Aged Ti-Mo Alloy

Yoshito TAKEMOTO*, Moritaka HIDA* and Akira SAKAKIBARA*

(Received February 7, 1996)

SYNOPSIS

The mechanism of brittle fracture in Ti-14mass%Mo alloy aged for 1×10^6 s at 623K was studied using transmission electron microscopy (TEM) and dynamic hardness test (DHT) on the structure deformed by means of tensile elongation at elevated temperature or cold rolling. Many band products were observed by TEM in either deformed specimens. These band products were identified to neither slips nor twinning bands, moreover, they were different from α , α' and α'' phases. The band product consisted of β phase and granular unknown phase which was transformed by deformation from ω phase. The newly discovered phase, named β'' phase, in the band products had a body-centered triclinic structure. The β'' was similar to the ω zone with respect to the morphology and the concentration of Mo, but it resembled β in structure. The result of DHT on the band products and the matrix showed that the band products were softer than the matrix. It is suggested that the band products are easily deformed because of the disappearance of obstacles such as ω phase, and consequently behave like paths to lead cracks preferentially.

1. INTRODUCTION

It is well known that the metastable β -titanium alloys become markedly brittle, caused by formation of ω phase, depending on aging treatments.⁽¹⁻⁵⁾ However mechanism of the brittle fracture has not been made clear yet. Previously we pointed out that brittle fracture in this alloy was microscopically caused by local softening of specimen, which was related to the inverse transformation from ω to β brought about by passing of partial dislocations.⁽¹⁾ In the present study microstructure and micromechanical properties were investigated to ascertain the relation between ω phase and brittle fracture.

2. EXPERIMENTAL

The tensile specimens were cut out by an electric spark cutter from a sheet of Ti-14mass%Mo alloy. These specimens were heated for 3.6ks at 1223K under a vacuum, then quenched into an iced water, and were subsequently aged for 1×10^6 s at 623K under a vacuum in order to make them brittle due to formation of ω phase. After heat treatment these specimens were mechanically ground and electrolytically polished at 223K in a solution of perchloric acid, n-butyl alcohol and methyl alcohol (v.f.=1:6:10). Tensile tests were carried out at temperatures between room temperature and 723K in an Ar atmosphere at a strain rate of 5.6×10^{-4} s⁻¹ until fracture. Rolling was done at room temperature to investigate the effect of cold work on the ω phase. Chemical etching was done by using a solution of equal parts water, nitric acid and hydrofluoric acid to examine the features of deformation products. Dynamic hardness was measured by Shimadzu DUH-201 in order to examine the differences of mechanical properties between the matrix and the deformation products. Thin foils suitable for TEM were prepared from deformed part of the specimens by an ion milling technique. The microstructure and composition analysis were performed by Topcon EM-002B with Kevex EDS system operated at 200kV.

* Department of Mechanical Engineering

3. RESULTS

Fig.1 shows nominal stress–strain curves at various temperatures of the specimen aged for 1×10^6 s at 623K. Both A and B curves represent brittle behavior at low temperature because of ω formation in the long time aging. As temperature of test increased, the tensile property became ductile as indicated by C and D. Electron fractography showed that failure occurred by dimple rupture in all cases, the dimple size decreasing with decreasing tensile temperature.

Fig.2(a) shows the typical optical micrograph of the specimen deformed at 723K in tension. There were many coarse traces similar to the slip lines. Several cracks were also observed in the coarse traces. It was found that the width of the deformation traces decreased with decrease of tensile temperature. Subsequently this specimen was mechanically and electrolytically polished to remove these deformation traces, then chemically etched. If these traces were slip lines, they should not reappear by the treatment. **Fig.2(b)** shows the same specimen as **Fig.2(a)** etched after polishing to remove the traces. Many traces reappeared, suggesting that they were different from common slip lines.

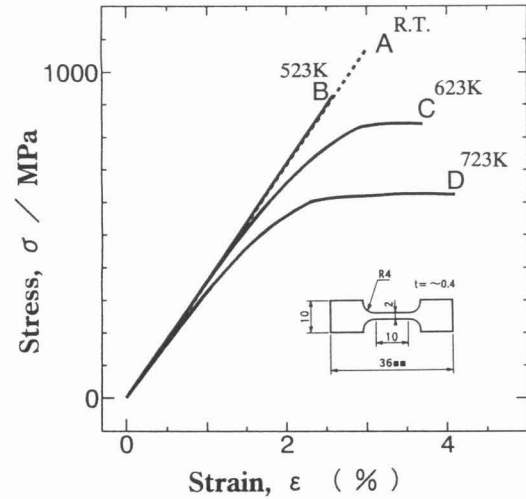


Fig.1 Stress–strain curves of aged Ti–14Mo alloy specimens deformed at various temperatures. (A) 300K, (B) 523K, (C) 623K and (D) 723K.

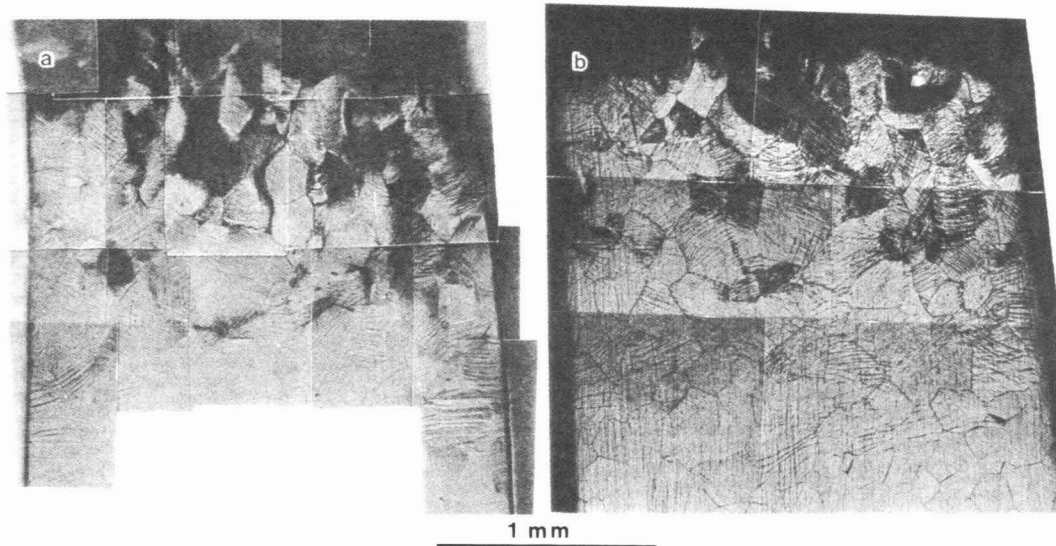


Fig.2 (a)Optical micrograph of a specimen deformed in tension at 723K. (b)The same specimen as (a) etched after polishing to remove deformation traces of (a).

The same result was obtained by the treatment on the specimen deformed by rolling at room temperature.

Fig.3 shows TEM micrograph of the same specimen as **Fig.2**. Many band products can be seen corresponding to the coarse traces shown in **Fig.2**. Generally the band products had a weak contrast, so that they became indistinguishable from the matrix by tilting of sample slightly. Selected area diffraction (SAD) patterns were taken from both the band product and the adjacent matrix.

Fig.4(a) shows the bright field (BF) image of a band product, and (b) and (c) show the SAD patterns having $[110] \beta$ zone axis taken from the matrix and the product marked by "b" and "c" in (a), respectively. In the matrix the ω reflections can be clearly seen in (b); on the other hand they are faint in the product, and unknown reflections indicated by an arrow in (c) appear. In contrast with (b), all reflection spots in (c) are arcing. It suggests that the band products contribute to deformation.

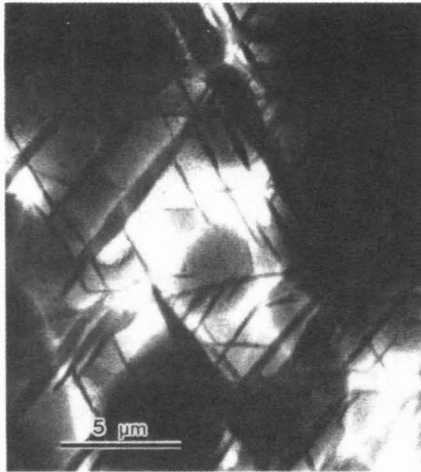


Fig.3 TEM microstructure of a specimen deformed at 723K, showing many band products.

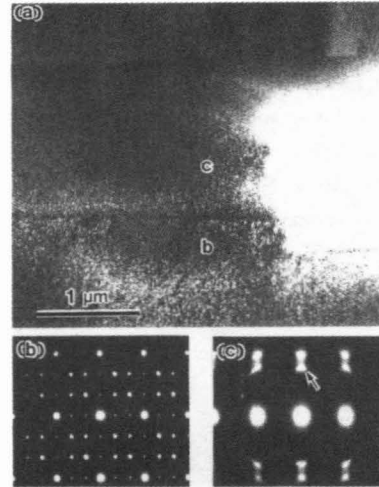


Fig.4 (a)The band product taken from $\langle 110 \rangle_{\beta}$.
 (b)SAD pattern of the matrix marked by "b" in (a).
 (c)SAD pattern of the band marked by "c" in (a).
 An arrow indicates the unknown phase.

Fig.5 shows the dark field (DF) images and SAD patterns having $[120]_{\beta}$ zone axis. The SAD pattern taken from the matrix indicates coexistence of β and ω phases in (a). The DF image of (b) using an ω reflection indicated by an arrow in (a) shows the disappearance of ω particles in the band product. The SAD pattern taken from the band product in (d) shows the disappearance of ω reflections, and appearance of unknown reflections indicated by an arrow. Fig.5(e) is the DF image of the same area as (b) using the unknown reflection. Many granular zones, of which the morphology and size are similar to the ω particles, can be seen just in the band product. However the shape of the granular zones is a little different from the ω particles. Fig.5(c) and (f) are enlargements of (b) and (e), respectively, and corresponding position is indicated by an arrow in photograph. The ω particles are ellipsoidal, having clear and smooth interface, while the interface of granular zones are blurred, having many striations within. It was also found by EDS analysis that the granular zone contained 10mass%Mo and the ω particle 7mass%Mo. Both compositions were much lower than the average one of this alloy.

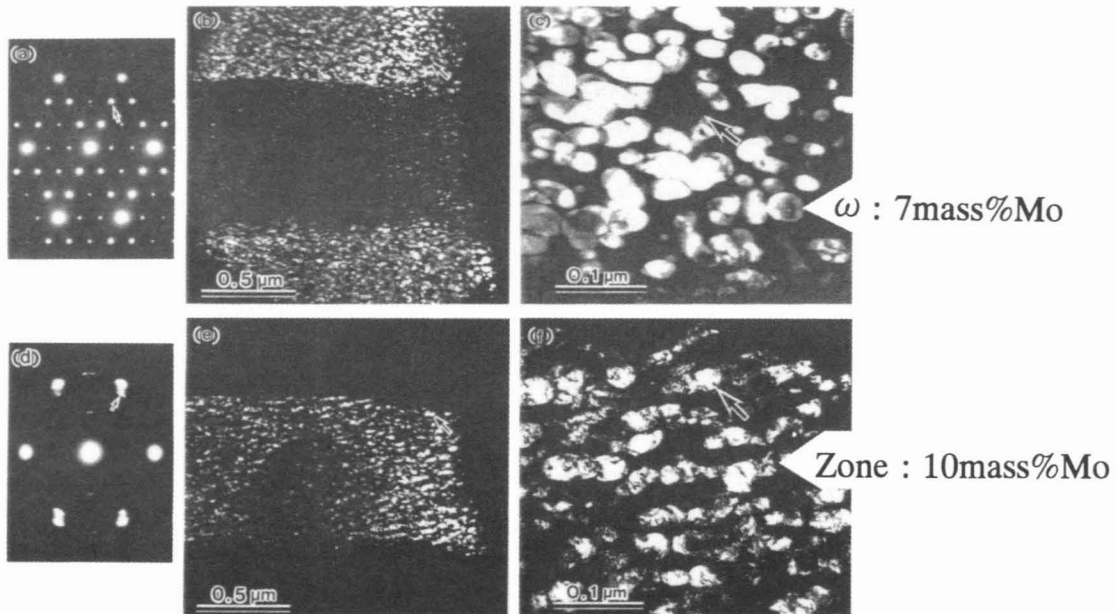


Fig.5 (a)SAD pattern of matrix, $\langle 120 \rangle_{\beta}$ zone axis. (b) and (c) are DF images using an ω reflection indicated by an arrow in (a). Arrows in (b) and (c) indicate the identical position. (d)SAD pattern of the band. (e) and (f) are DF images using a reflection indicated by an arrow in (d). Arrows in (e) and (f) indicate the identical position.

Fig.6(a) shows TEM micrograph of the specimen rolled to about 10% reduction in thickness at room temperature. There are two types of band product in elongated direction. **Fig.6(b)**, (c) and (d) are SAD patterns taken from respective regions marked by letters of b ~ d in (a). In the matrix β and ω reflections can be seen in (b), but ω reflections disappear in the band products of "c" and "d". The SAD patterns of **Fig.6(d)** and **Fig.4(c)** resemble each other. Consequently it is considered that the band products produced either at 723K or at room temperature are essentially the same.

There are two types of SAD pattern in the band products; the one exhibiting a single β pattern in appearance as shown in **Fig.6(c)**, and the other representing a pattern quite different from β matrix as shown in **Fig.6(d)**.

To examine the difference in mechanical properties between the matrix and the band product on the specimen deformed at 723K in tension, dynamic hardness test (DHT) was carried out using a trigonal-pyramidal indenter with a load of 1gf at room temperature. Hardness was measured at more than eight points in each region, and the average was shown in **Fig.7**. It was found that the band products were certainly softer than the matrix containing ω phase.

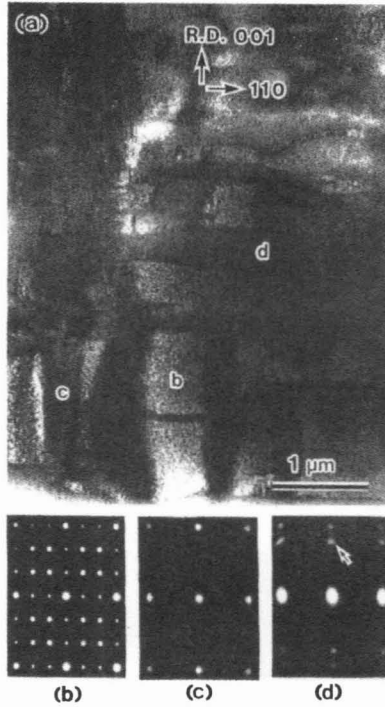


Fig.6 (a)TEM micrograph of a rolled single crystal.
(b)–(d) show SAD patterns taken from the different regions in (a).

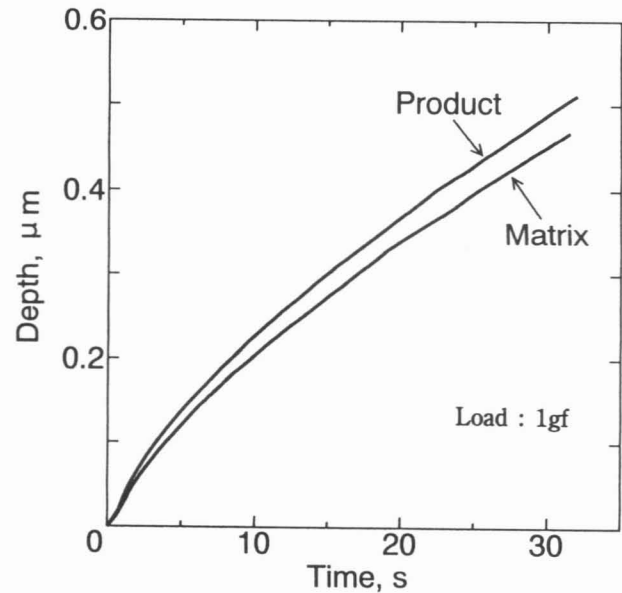


Fig.7 Dynamic Hardness of band product and matrix of the specimen deformed at 723K in tension, showing the band product is softer than the matrix.

4. DISCUSSION

4.1. Unknown phase in the band product

The band product observed in this study does not correspond to anything reported so far; e.g. α , α' , α'' , twin and common slip band. It consists of β phase and unknown phase similar in configuration, size and composition to the ω phase. It is considered that the unknown phase has been transformed from ω phase, induced by deformation. To identify the structure of the unknown phase, computer calculation was carried out based on the SAD patterns taken from the band products. As a result of calculation it was found that the body-centered triclinic structure ($a=0.310\text{nm}$, $b=0.310\text{nm}$, $c=0.375\text{nm}$, $\alpha=96^\circ$, $\beta=90^\circ$ and $\gamma=94^\circ$; $\Delta V/V_\beta=+4.15\%$) was the most reasonable for the phase as shown in **Fig.8**. Though not exactly proper for crystallographic terminology, such notion is suitable for comparing it with β phase. Since it was similar to the β phase rather than ω phase in structure, it was named β'' phase. Orientation relation between β and β'' was approximately as follow; $(110)\beta // (110)\beta''$, $[110]\beta // [110]\beta''$. As a result from trace analysis the shape of band product itself was a plate which habit plane was

near $\{001\} \beta$ or $\{110\} \beta$.

Fig.9 shows two types of probable mechanism in β'' transformation from ω phase. When ω is sheared by successive partial dislocations, the ω inversely transforms to β structure as shown in Fig.9(a), subsequently goes on transforming to the β'' structure. Such a zone has a composition inherited from ω phase, and has a close orientation relation to the β matrix, which we will call β''_N . On the other hand if the β'' transformation is completed by passing the partials in the opposite direction as shown in Fig.9(b), that zone has a $\{112\}$ twin relation to the β''_N , which we will call β''_T . As mentioned earlier, two types of SAD pattern of the band products are dependent on whether the band contains β''_N or β''_T zones. If β twin zone in Fig.9(b) is observed from the direction indicated by an arrow, its orientation will be parallel to $[110] \beta$ of matrix and to $[114] \beta$ of twin zone which is close to $[001] \beta$, twin direction with difference angle of about 19° . Moreover the angle difference will decrease by transformation from β twin to β''_T zone. Consequently the pattern of Fig.6(d) can be explained as a combination of both $(110) \beta$ and $(001) \beta''_T$ patterns. For all SAD patterns of the band products including those unpublished here we have succeeded in explanation by using either β''_N or β''_T .

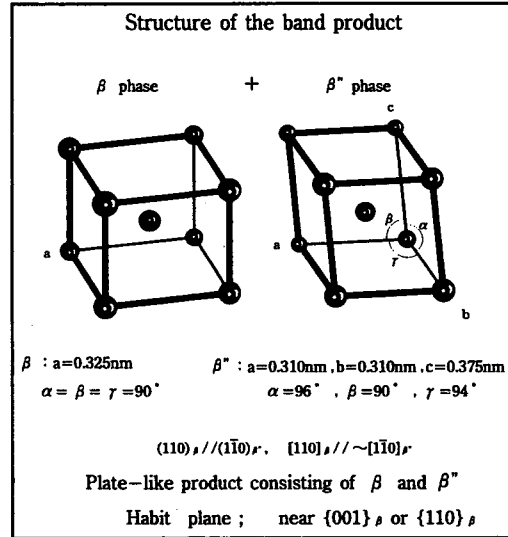


Fig.8 Structure of β'' phase, and orientation relation between β and β'' . The band product consists of β and β'' particles.

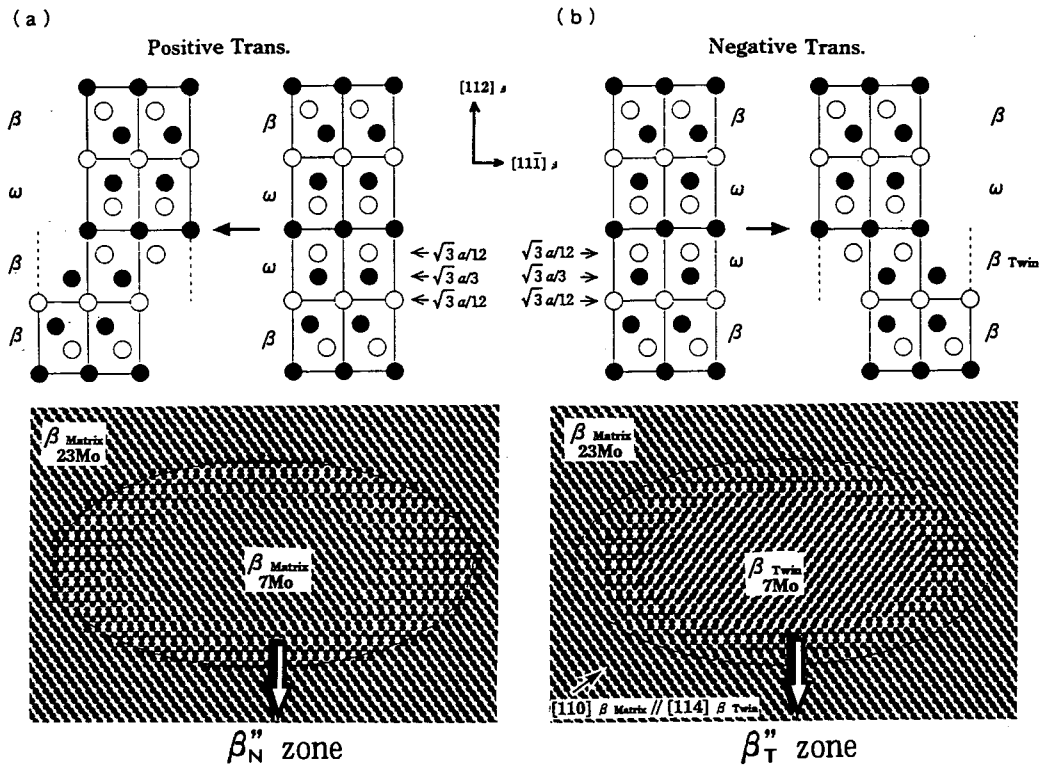


Fig.9 Schematic diagrams of the inverse transformation from ω to β . The upper diagrams are two types of transformation sequences, (a)positive, (b)negative transformation. The plane normal is $[110] \beta$ direction. Open circles represent atoms in the plane, and solid circles are atoms out of the plane. The lower diagrams are the computed atomic arrangement of the transformed region. Positively transformed region is conformably related with the matrix. Negatively transformed region is $\{112\} \langle 111 \rangle$ twin-related with respect to the matrix.

4.2. Brittle fracture mechanism

There have been attempts in the past to understand the brittle nature of β alloys containing the ω phase. ⁽¹⁻⁵⁾ However two difficulties to explain the mechanism have been encountered. Firstly, even macroscopically brittle samples fail by a localized but ductile fracture mode, showing the dimpled structure in fractography. ⁽³⁾ Secondly, in shearing mechanism of ω particle a $\langle 111 \rangle$ slip direction of β is convenient for a given ω phase to deform but it is not suitable for other three ω variants. ⁽²⁾ The band products discovered in this study would give a key to solve the first question. **Fig.10** shows the schematic sequence of brittle fracture in aged Ti-Mo alloy containing ω particles. The ω variants in the band change to β'' phase expected to behave very similarly to β phase in deformation mode, β'' zones will not operate to obstruct dislocation movement as ω particles do. The result of DHT gives an evidence in support of this consideration. Slips therefore concentrate and lead crack propagation within the band; finally the failure occurs with no macroscopic plastic strain, but it will exhibit ductile fracture mode with small dimples. It is considered that the dimple size in the fracture surface correlates with the width of band product, that is, the decrease of dimple size with decrease of tensile temperature is corresponding to the decrease of width of the band produced.

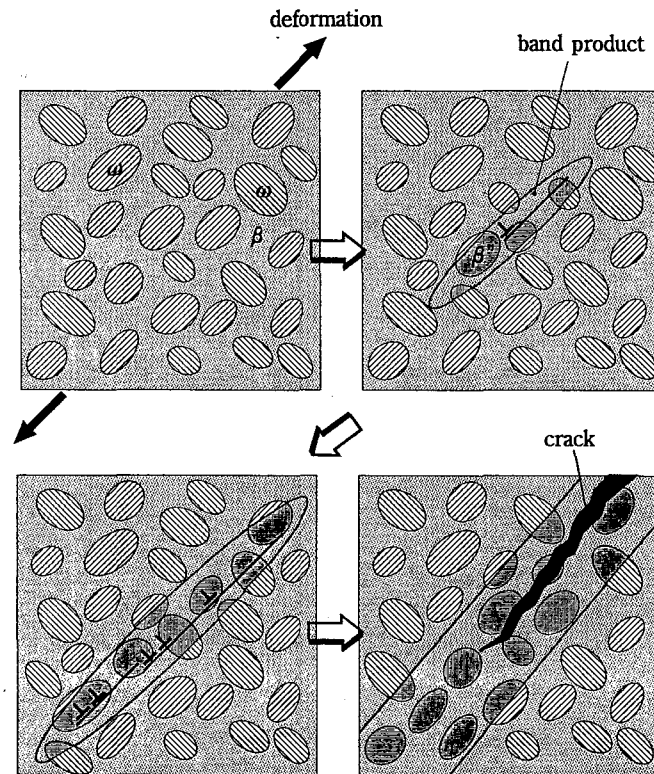


Fig.10 Schematic illustration of brittle fracture in aged Ti-Mo alloy.

While the second question has not been completely answered at present, it is reasonable to expect that a given Burgers vector of $1/2[111] \beta$, which enables an ω phase to deform, can be resolved into three vectors of $1/2\langle 111 \rangle \beta$ not parallel each other, by which other three ω variants are deformable and transformable to either β''_N or β''_T . According to the destruction of all the four ω variants the transformed region will not have a simple $\{112\} \beta$ habit plane but have a $\{001\} \beta$ plane composed of the four $\{112\} \beta$ planes corresponding to the deformation of four ω variants. As reported in the previous paper, single crystal sample of Ti-14mass%Mo alloy aged for 1×10^5 s at 623K and elongated at room temperature resulted in complete embrittlement having macroscopic $\{001\} \beta$ fracture surface; however the surface microscopically consisted of two $\{112\} \beta$ planes containing small dimples. ⁽¹⁾ It suggests that $\{112\}\langle 111 \rangle$ slips can operate within the band product and that the brittle fracture in aged β -titanium alloys results from by a restriction of deformable region.

5. CONCLUSIONS

Brittle fracture mechanism of Ti–14mass%Mo alloy aged for long time was investigated with relation to deformation products. The results can be summarized as follows:

- (1) In the band products generated by deformation the ω phase transforms to the β'' phase which is similar to the β phase in structure. The band product is plate shaped having near $\{001\}$ β or $\{110\}$ β habit plane, and consists of β and β'' phases.
- (2) There are two types of β'' phase, different in orientation relation to the β matrix caused by difference in transformation process.
- (3) The band product is easier to deform plastically than the matrix containing ω phase, and behaves like a path to lead crack preferentially.
- (4) Brittle fracture in this alloy is caused by the intense $\{112\}\langle 111\rangle$ slips within the band.

ACKNOWLEDGMENTS

The authors gratefully acknowledge the assistance of Messrs. S.Ibaraki, H.Shinkai, T.Tanaka and H.Morisaki. They would like to thank Cooperative Research Center Okayama University for using HR–TEM and also thank Okayama Prefectural University for study of DHT. This work has been supported by the Grant–in–Aid for Scientific Research for the Ministry of Education, Science and Culture, Japan.

REFERENCES

- (1) Y.TAKEMOTO, M.HIDA, E.SUKEDAI and A.SAKAKIBARA: J. Japan Inst. Metals, **53**(1989) 1004–1012.
- (2) J.M.SILCOCK: Acta Met., **6**(1958) 481–493.
- (3) J.C.WILLIAMS, B.S.HICKMAN and H.L.MARCUS: Met. Trans., **2**(1971) 1913–1919.
- (4) T.W.DUERIG, G.T.TERLINDE and J.C.WILLIAMS: Met. Trans., **11A**(1980) 1987–1998.
- (5) G.T.TERLINDE, T.W.DUERIG and J.C.WILLIAMS: Met. Trans., **14A**(1983) 2101–2115.